

# Slow Infrared Laser Dissociation of Molecules in the Rapid Energy Exchange Limit<sup>†</sup>

Kolja Paech, Rebecca A. Jockusch, and Evan R. Williams\*

Department of Chemistry, University of California, Berkeley, California 94720

Received: January 9, 2002; In Final Form: May 9, 2002

An improved model for the slow infrared laser photodissociation of large biomolecules is proposed. As has been previously shown by master equation and Monte Carlo calculations, large, laser-heated molecules reach steady-state internal energy distributions that very closely approximate Boltzmann internal energy distributions. By approximating the internal energy distribution of laser-heated molecules as a Boltzmann distribution, one can derive a very simple relationship between the relative laser power experienced by the ions and the ion temperature. This relationship can be substituted into the Arrhenius equation, yielding a new Arrhenius-like relationship for slow laser dissociation. The model presented here is a modified version of the laser dissociation model proposed by Dunbar in 1991 (*J. Phys. Chem. A* 2000, 104, 3188–3196). Dunbar's model, while making the correct qualitative predictions, significantly underestimates the activation energy of large molecules measured by laser dissociation. The present laser dissociation model differs from the Dunbar model in that stimulated and spontaneous emission at all frequencies is included in the analysis. A significant result of this model is that there is a parametrized relationship between the laser power and the dissociation rate constant and that the parametrization for different classes of polymers can be determined computationally. This new model gives activation energies via CO<sub>2</sub> laser dissociation that are in good agreement with activation energies measured by blackbody infrared radiative dissociation.

## Introduction

Blackbody infrared radiative dissociation (BIRD) can provide accurate information about ion dissociation energetics for a wide range of molecules.<sup>1–15</sup> In a BIRD experiment, ions exchange energy with the blackbody field generated within a uniformly heated vacuum chamber of a Fourier transform ion cyclotron resonance (FT-ICR) mass spectrometer. Because the mechanism of energy exchange of the ions is well-characterized and because the photon intensity distribution within the heated vacuum chamber is known, the BIRD dissociation process can easily be modeled. Small ions, which have few vibrational modes and exchange energy with the radiation field relatively slowly, do not reach a true equilibrium (Boltzmann) internal energy distribution in a BIRD experiment. Therefore, numerical modeling of the dissociation process is needed to evaluate experimental data because direct application of the Arrhenius equation provides parameters that are too low.<sup>4–7</sup> Large ions exchange energy with the blackbody radiation field rapidly enough to maintain a Boltzmann internal energy distribution during dissociation. In this limit of rapid energy exchange, BIRD measurements yield activation energies via a direct application of the Arrhenius equation that are equivalent to activation energies measured by high-pressure methods.<sup>5–9</sup>

Photodissociation using a cw-CO<sub>2</sub> laser, a method pioneered by Beauchamp and co-workers for the study of small ions,<sup>16,17</sup> offers two significant advantages over BIRD. Much higher ion internal energies can be achieved using a CO<sub>2</sub> laser, making possible the dissociation of molecules that are too stable to dissociate at the highest temperatures accessible in a typical BIRD experiment. Also, CO<sub>2</sub> laser dissociation is a much faster technique than BIRD because CO<sub>2</sub> laser dissociation does not require a lengthy temperature equilibration of the instrument

vacuum chamber. A significant limitation of the slow laser heating method has been an inability to obtain accurate quantitative thermodynamic values. This is primarily due to the difficulty of characterizing the internal energy distribution of the dissociating ion population.

In 1991, Dunbar proposed a thermal dissociation model for the slow laser heating of molecules.<sup>18</sup> One of the fundamental assumptions of the Dunbar model is that laser-heated molecules exchange energy exclusively via their vibrational mode or modes at the laser frequency. Using this assumption, Dunbar derived a simple relationship between the relative laser intensity and the ion temperature, which could be substituted into the Arrhenius equation. Dunbar showed that characterization of the laser-heated population by a temperature was valid because random-walk simulations for *n*-butylbenzene showed that the internal energy distribution of the slowly dissociating ion population was essentially a Boltzmann distribution. Dunbar's thermal equivalence model was applied to the dissociation of two small molecules, *n*-butylbenzene and styrene, yielding a reasonable prediction (within 30%) of the laser-intensity dependence of the dissociation rate.<sup>19,20</sup>

Freitas et al. applied Dunbar's model to the CO<sub>2</sub> laser dissociation of bradykinin<sup>21</sup> and bovine ubiquitin.<sup>22</sup> For ubiquitin, these authors found that the model yields correct relative activation energies for two different charge states of this protein.<sup>22</sup> However, these authors found that Dunbar's model gives activation energy values for the dissociation of peptides and proteins that are about 40% lower than those measured using BIRD. Judging from this result, Freitas et al.<sup>22</sup> suggested that Dunbar's model might be improved by incorporating an empirical scaling factor for the activation energy determined by comparison to BIRD values.

The accuracy of dissociation energies measured by CO<sub>2</sub> laser dissociation can be improved by fitting experimental data to master equation calculations.<sup>23</sup> For protonated leucine enkepha-

<sup>†</sup> Part of the special issue "Jack Beauchamp Festschrift".

\* To whom correspondence should be addressed.

lin, Jockusch et al.<sup>23</sup> demonstrated that the dissociation energy measured using this approach was consistent with, although less precise than, the value obtained using BIRD. Here, we present a model that is much simpler to apply to laser-dissociation experiments than a full master equation analysis and yet appears to yield accurate activation energies. Our modified model does not use the assumption of the original Dunbar model that a laser-heated molecule exchanges energy only through its laser-frequency vibrational mode. This model is successfully applied to previously published laser dissociation data<sup>21–23</sup> and to new measurements of the CO<sub>2</sub> laser dissociation of singly and doubly protonated bradykinin and doubly and triply protonated melittin.

## Experimental Methods

**Instrumentation.** Experimental measurements were made using a 2.7-T Fourier transform mass spectrometer that has been described in detail previously.<sup>9</sup> A 25-W cw-CO<sub>2</sub> laser (model 48-2-28W, Synrad Inc., Bothell, WA) was used to dissociate the ions. Details of the laser setup have been published previously.<sup>23</sup> No modifications to the setup in ref 23 were made for the bradykinin and melittin dissociation experiments described here.

**Dissociation Experiments.** Ions are generated using home-drawn borosilicate capillaries for nanoelectrospray ionization. The ions are brought from atmospheric pressure to about  $5 \times 10^{-9}$  Torr through five stages of differential pumping and guided to the ion cell via a series of electrostatic lenses. Ions are trapped with trapping plates set at 5 V and nitrogen trapping gas at a background pressure of about  $2 \times 10^{-6}$  Torr. The load time is adjusted to maximize the ion signal. A 2-s pump-out delay follows the closing of the pulsed valve that is used to introduce the nitrogen gas. Trapped ions are isolated via a combination of RF waveforms. Ions are subsequently irradiated with the CO<sub>2</sub> laser using radiation intensities between  $\sim 5$  and  $50 \text{ W/cm}^2$ . Ions are excited for detection via a broadband chirp excitation with a sweep rate of 951 kHz ( $m/z$  90 cutoff) on an Odyssey data collection system (Finnigan, Madison, WI). The ion abundances were measured relative to a stable single-frequency radio signal at 331 MHz. The kinetic data were obtained from single measurements unless otherwise noted.

**Materials.** Bradykinin and melittin were purchased from Sigma Chemical Company (St. Louis, MO) and used without further purification. Electrospray solutions were  $\sim 5 \times 10^{-5}$  M in the analyte species in a 50:50 water/methanol solution containing  $\sim 1\%$  acetic acid.

**Master Equation Model.** The master equation program used to calculate the internal energy distributions of laser-heated leucine enkephalin (LE) has been previously described in detail.<sup>23</sup> In this model, the laser emission is modeled as a 9.1-mm-diameter beam with a  $100 \text{ cm}^{-1}$  wide flat-topped intensity and spectral distribution. The exaggerated width of the emission wavelength window was adopted to address the uncertainties in AM1-calculated frequencies within the laser emission window.<sup>23</sup> For the present study, only the relative laser intensity is important, and therefore, the existing laser dissociation code was used without modification. Calculations for the laser heating of leucine enkephalin in the zero-dissociation limit were performed with master equation program variables as described previously (laser beam diameter, 9.1 mm; laser beam attenuation, 31%; and transition dipole multiplying factor, 1.8).<sup>23</sup> For the RRKM calculation of leucine enkephalin (LE), the transition-state frequency set was constructed from the reactant frequency set of leucine enkephalin as follows: one frequency (a C–C stretch at  $1329 \text{ cm}^{-1}$ ) was removed as the dissociation coordi-

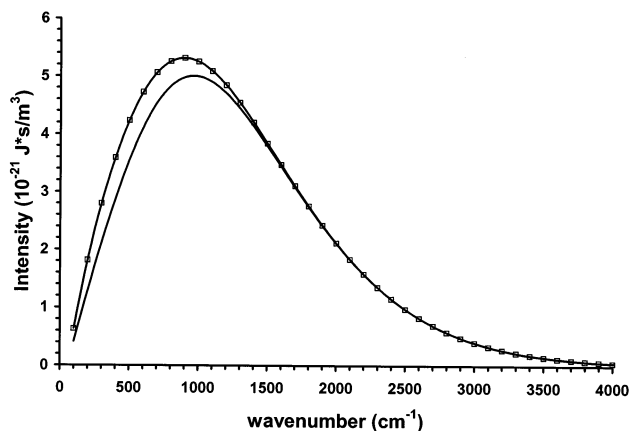


**Figure 1.** Relative emission intensities for oscillators with a normalized transition dipole moment. Relative emission is calculated under the assumption that vibrational levels are populated according to canonical single harmonic oscillator probabilities. The upper curve (open squares) represents the relative emission from a 500 K population and a background temperature of 500 K. The lower curve (solid line) represents the relative emission from a 500 K population in a 298 K Planck distribution.

nate, and five other frequencies were modified to construct a transition-state frequency set with an Arrhenius  $A$  factor of 10.74. The threshold dissociation energy of LE was set to an artificially high value of 1.98 eV to model an ion population that has equilibrated with the laser beam but does not dissociate on the time scale of the experiment.

## Model for the Laser Dissociation of Large Molecules

**Laser Heating of Molecules.** Many gas-phase molecules and ions dissociate at rates measurable by Fourier transform ion cyclotron resonance mass spectrometry at temperatures between 400 and 600 K. At these temperatures, high-frequency vibrational modes are essentially frozen out and, therefore, do not emit significantly. Because the power dissipated by a vibrational mode decreases as  $\nu^3$ , the relative emission intensity (at constant transition dipole moment) peaks in the mid-IR range near  $1000 \text{ cm}^{-1}$ . Because of this, Dunbar made the approximation that a laser-heated ion emits only at the laser frequency if this frequency is near  $1000 \text{ cm}^{-1}$  (such as a CO<sub>2</sub> laser at  $943 \text{ cm}^{-1}$ ). However, this approximation can lead to significant errors because the relative emission does not peak *sharply* in the mid-IR region. Figure 1 shows the relative emission intensities for oscillators with the same transition dipole moment for a 500 K population in Planck background temperatures of both 500 and 298 K. Intense transitions several hundred wavenumbers higher or lower than  $1000 \text{ cm}^{-1}$  will still make a significant contribution to a molecule's total emission, and as we will show, neglecting vibrational modes higher and lower than the laser frequency can lead to significant errors.

A molecule's stimulated emission at the laser frequency ( $943 \text{ cm}^{-1}$ ) is much higher when it is laser-heated than when it is heated by a blackbody field in a BIRD experiment because of the high power density at the laser frequency. However, at the laser intensities generally employed for slow CO<sub>2</sub> laser dissociation of peptides and proteins ( $5\text{--}75 \text{ W/cm}^2$ ), the stimulated emission at the laser frequency is at most 750 times higher than the spontaneous emission at the laser frequency. In the Dunbar model, it is assumed that an ion's total emission can be approximated by the stimulated emission at just the laser frequency. Although this assumption might be a reasonable approximation for small molecules, it can lead to significant

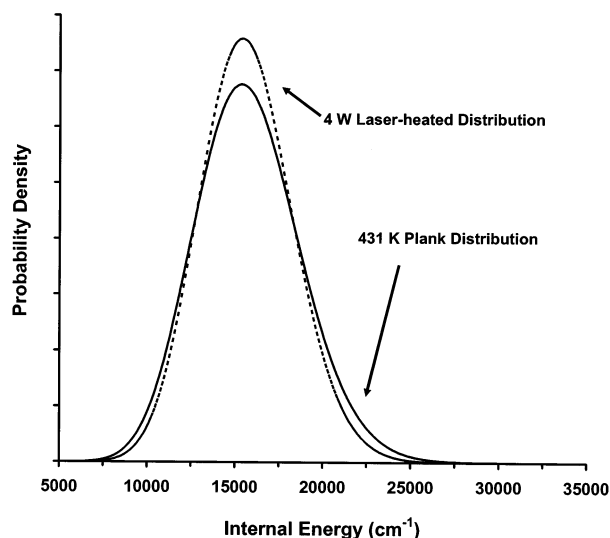


**Figure 2.** Comparison of the internal energy distribution for a nondissociating population of protonated leucine enkephalin in a laser heating experiment (room-temperature Plank distribution with 4-W laser beam). Also shown is a Boltzmann internal energy distribution for this same ion at 431 K.

errors for large molecules. The energy loss from spontaneous emission from all of the non-laser-frequency vibrational transitions can easily exceed that from stimulated emission at the laser frequency. Not only are there many more vibrations at frequencies other than the laser frequency, but the transition dipole moments of these vibrations can be much more intense (by a factor of 10–100 or more for peptides) than the transition dipole moment at the laser frequency.

One way to take the overall emission behavior of a laser-heated molecule into account is to perform a complete master equation calculation.<sup>23</sup> Although this is straightforward (but tedious) for smaller molecules, extending master equation calculations to proteins is computationally difficult. For cases in which the internal energy distribution of the dissociating ion population is Boltzmann-like, mathematical modeling of laser dissociation can be greatly simplified. One situation in which this appears to be the case is slow CO<sub>2</sub> laser dissociation, which has been shown to result in a dissociating steady-state population that very closely resembles a Boltzmann distribution, even for relatively small molecules.<sup>16,22,23</sup>

Our master equation modeling program for CO<sub>2</sub> laser dissociation was used to generate internal energy distributions in the zero-dissociation limit for leucine enkephalin (Figure 2). In these calculations, the threshold dissociation energy was set artificially high (1.98 eV) to determine what the internal energy distribution would look like in the limit of rapid energy exchange. The motivation for these calculations was to probe qualitatively the internal energy distribution of large laser-heated molecules, because the fundamental difference between the laser heating of smaller and larger peptides is their rate of exchange of photons. As can be seen in Figure 2, the internal energy distribution of a peptide in the rapid energy exchange limit is only slightly narrower than a true Boltzmann distribution.

**Laser Power and Molecule Temperature.** To describe laser dissociation by simple equations analogous to the Arrhenius equation, we must derive a relationship between the laser power and the thermal equilibrium variable, the temperature  $T$ . When an ion population reaches a steady state, its net absorption must be zero in the absence of dissociation. In the first approximation, one can neglect the net absorption of a steady-state ion population when its rate of dissociation is very slow. Thus, for

a molecule whose interaction with the radiation field is described by a simple coupled harmonic oscillator model, the steady-state condition is given by eq 1

$$\sum_{\nu} B(\nu) \rho(\nu) P(\nu) = \sum_{\nu} [A(\nu) + B(\nu) \rho(\nu)] P''(\nu) \quad (1)$$

In eq 1, the right-hand side represents the emission and the left-hand side represents the absorption.  $A(\nu)$  and  $B(\nu)$  are the Einstein  $A$  and  $B$  coefficients, respectively, for the transition between the ground and first excited vibrational levels of vibrational mode  $\nu$ , and  $\rho(\nu)$  is the energy density at frequency  $\nu$ .  $P(\nu)$  and  $P''(\nu)$  include the occupation probability of all excitation levels,  $n$ , ( $n = 0, 1, 2, \dots$ ) of vibrational frequency,  $\nu$ , and the increased probability of absorption and emission as a function of  $n$ . When the internal energy distribution of the laser-heated molecules can be approximated as a Boltzmann distribution (that is, when the ion population can be characterized by a temperature  $T$ ), then  $P(\nu, T)$  and  $P''(\nu, T)$  are given by eqs 2 and 3, respectively

$$P(\nu, T) = \sum_{n=0}^{\infty} e^{-nh\nu/kT} (1 - e^{-h\nu/kT}) (n + 1) \quad (2)$$

$$P''(\nu, T) = \sum_{n=0}^{\infty} e^{-nh\nu/kT} (1 - e^{-h\nu/kT}) n \quad (3)$$

In these equations, the terms  $(n + 1)$  and  $(n)$  are the squares of the creation and annihilation operators, respectively. Physically, they represent the increased absorption and emission probabilities for higher occupation levels of a vibrational mode. The product of the two terms containing exponentials in eqs 2 and 3 is the occupation probability for a simple harmonic oscillator of frequency  $\nu$  in its  $n$ th excited state in a thermal distribution at a temperature  $T$ . The summation over all  $n$  takes into account all possible excitation states of an oscillator with frequency  $\nu$ .

We wish to find a simple relationship between the laser power and the ion temperature. To arrive at such a relationship, we must isolate the laser power from eq 1. Rearranging eq 1 by combining the summations, we arrive at eq 4

$$0 = \sum_{\nu} \{A(\nu) P''(\nu) + B(\nu) \rho(\nu) [P''(\nu) - P(\nu)]\} \quad (4)$$

As a first simplification, one can make use of the fact that  $P(\nu, T) - P''(\nu, T) = 1$ , yielding

$$0 = \sum_{\nu} [A(\nu) P''(\nu) - B(\nu) \rho(\nu)] \quad (5)$$

Now, one can remove only the laser-frequency vibrational mode from the summation, giving

$$0 = A(\nu_{\text{laser}}) P(\nu_{\text{laser}}) - B(\nu_{\text{laser}}) \rho(\nu_{\text{laser}}) + \sum_{\nu'} [A(\nu') P(\nu') - B(\nu') \rho(\nu')] \quad (6)$$

In eq 6, the summation is over all frequencies  $\nu'$  except the laser frequency,  $\nu_{\text{laser}}$ . Rearranging eq 6 by isolating the laser-frequency energy density yields

$$\rho(\nu_{\text{laser}}) = -\frac{1}{B(\nu_{\text{laser}})} \left\{ \sum_{\nu'} [B(\nu') \rho(\nu') - A(\nu') P(\nu', T)] - A(\nu_{\text{laser}}) P''(\nu_{\text{laser}}, T) \right\} \quad (7)$$

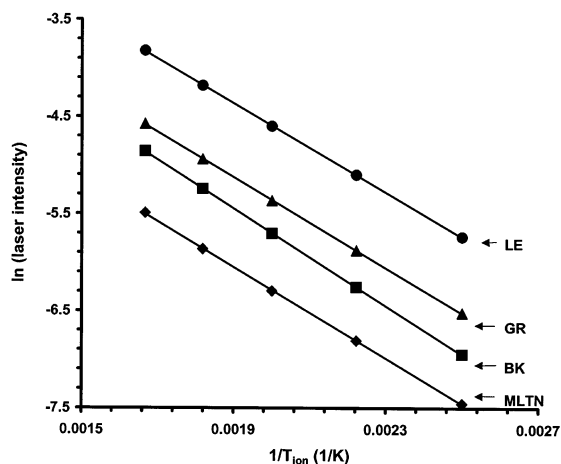


**Figure 3.** Calculated relationship between the relative laser intensity and the ion internal temperature based on AM1-generated frequencies and intensities for four peptides: LE (triangles, leucine enkephalin), GRS (squares, gramicidin S), BK (diamonds, bradykinin), and MLTN (circles, melittin).

Unlike the Dunbar model, no simple analytical relationship exists between the laser power and the ion temperature. However, given any absorption spectrum, one can easily calculate the laser power that will bring an ion population to a temperature  $T$  under the assumption of complete thermal equilibration.

Ideally, one would like to be able to solve eq 7 for the full calculated vibrational spectrum of a molecule. In practice, this is complicated by the large number of vibrational frequencies for larger peptides. To simplify this calculation, the frequency sets used in the solution of eq 7 were averaged into  $100\text{ cm}^{-1}$  wide bins, making the calculation straightforward to accomplish in Mathematica (Wolfram Research, Champaign, IL). Averaging into  $100\text{ cm}^{-1}$  wide bins was done by adding the transition probabilities for all wavelengths within a  $100\text{ cm}^{-1}$  window and treating all wavelengths within that window as a single frequency at the central wavelength of that window. For instance, the squares of all transition dipole moments for all frequencies between  $100$  and  $200\text{ cm}^{-1}$  from a calculated frequency file were added and treated as the square transition dipole of a single frequency at  $150\text{ cm}^{-1}$ .

Absorption spectra for four peptides were calculated at the semiempirical AM1 level. Substitution of these frequencies and transition dipole moments (multiplied by 1.8)<sup>23</sup> into eq 7 using the simplifications explained above yields a linear relationship between the logarithm of the laser power and the reciprocal of the ion internal temperature, with a proportionality factor that we call  $s$  (Figure 3)

$$\frac{d \ln \rho(\nu_{\text{laser}})}{d(1/T)} = -s \quad (8)$$

where  $\rho(\nu_{\text{laser}})$  is the radiation intensity at the laser frequency and  $T$  is the ion internal temperature. The proportionality factor,  $s$ , has units of Kelvins. No significant difference in the calculated value of  $s$  was found by changing the bin width from  $100$  to  $400\text{ cm}^{-1}$ , and therefore, it appears that this slightly averaged calculation should yield a relationship nearly identical to that obtained with a more rigorous calculation in which each frequency is explicitly included.

The existence of a linear relationship between the logarithm of the laser power and the reciprocal of the ion internal temperature is very convenient in several ways. One problem

in relating the laser power to the unimolecular dissociation rate constant is that there is a significant uncertainty in the energy deposited into an ion with a  $\text{CO}_2$  laser because (a) the calculated Einstein  $B$  coefficient(s) for the laser-frequency transition(s) of the ion has (have) significant uncertainty, (b) the absolute laser intensity experienced by the ions is difficult to determine accurately, and (c) the absolute values of calculated frequencies and intensities are not highly accurate. In eq 8, the absolute laser power is irrelevant, because by differentiating the logarithm of the laser power, any scalar multipliers to the laser power are eliminated. Substitution of eq 8 directly into the Arrhenius equation therefore yields a relationship between the unimolecular dissociation rate constant ( $k_{\text{uni}}$ ) and the laser power that does not depend on the absolute laser power

$$\frac{d \ln k_{\text{uni}}}{d \ln \rho(\nu_{\text{laser}})} = \frac{E_a}{sk} \quad (9)$$

In eq 9,  $k$  is the Boltzmann constant, and all other terms are as previously defined. Taking the logarithm of both sides of eq 7 and differentiating with respect to  $1/T$  introduces a further simplification

$$\frac{d \ln \rho_{\text{relative}}(\nu_{\text{laser}})}{d(1/T)} = - \frac{d}{d(1/T)} \ln \left( \sum_{\nu} [B(\nu') \rho(\nu') - A(\nu') P''(\nu, T)] - A(\nu_{\text{laser}}) P''(\nu_{\text{laser}}, T) \right) \quad (10)$$

In eq 10,  $\rho_{\text{relative}}(\nu_{\text{laser}})$  is the relative laser power (because scalar multipliers are eliminated), and all other terms are as previously defined. By differentiating the logarithm of eq 7, the Einstein  $B$  coefficient at the laser frequency drops out of the right-hand side of the equation, leaving only the Einstein  $A$  coefficient at the laser frequency and Einstein  $A$  and  $B$  coefficients at all other frequencies to contribute to the value of  $s$ . As discussed later, changing the laser-frequency Einstein  $A$  coefficient results in an insignificant change in the calculated value of  $s$ . Unlike the Dunbar model, the present model predicts that the relationship between the unimolecular dissociation rate constant depends on the intensities of all vibrational frequencies of an ion and, in fact, depends significantly on the vibrational transitions not at the laser frequency. In this model, then,  $s$  is a broad average over the entire absorption and emission spectrum of an ion and local differences in an ion's absorption spectrum should lead to minor changes in  $s$ .

Another convenient consequence of eq 10 is that the proportionality constant,  $s$ , does not depend on the absolute intensity of vibrational transitions, but rather depends on the relative intensities of an ion's vibrational transitions. Therefore, if one multiplies the number of frequencies but keeps the frequency and intensity distributions the same (that is, if one multiplies absorption intensities by a scalar multiplier), the Arrhenius-like laser dissociation equation (eq 8) will be unchanged. Linear polymers are classes of molecules for which the above simplifications are especially relevant. The absorption spectrum of linear polymers changes primarily by increasing the number of vibrations as the polymer size increases while not significantly altering the relative absorption intensities. For various classes of linear polymers, such as peptides or oligonucleotides, it is likely that  $s$  will be the same for an entire class of molecules. This should make the analysis of laser dissociation data of ions within the rapid energy exchange limit very simple once the appropriate value of  $s$  for a given class of molecules has been established.

**TABLE 1: Calculated  $s$  Values for Four Peptides Obtained by Using the Summed Transition Dipole Moments for 100  $\text{cm}^{-1}$  Wide Wavelength Bins**

compound	mass (Da)	calculated value of $s$ (K)
leucine enkephalin	555	2348
bradykinin	1061	2339
gramicidin S	1241	2504
melittin	2845	2295
average		2369

The new laser dissociation model was applied to four peptides: leucine enkephalin, bradykinin, melittin, and gramicidin S. Values of  $s$  for each of these peptides determined from their calculated vibrational spectra (Figure 3) are given in Table 1. These values are all similar, deviating by less than 9% from each other. Because the value of  $s$  should not be a strong function of molecular size, the new laser dissociation model should be applicable to both peptides and proteins. The relationship between laser power and dissociation rate constant for polypeptides is given by eq 11

$$\frac{d \ln k}{d \ln \rho(\nu_{\text{laser}})} = 4.80E_a \quad (11)$$

where  $E_a$  is the activation energy for dissociation in electronvolts. In comparison, Dunbar's model (neglecting corrections for the truncation of the internal energy distribution, which are not part of the model presented in this paper) makes the following prediction

$$\frac{d \ln k_{\text{uni}}}{d \ln \rho(\nu_{\text{laser}})} = \frac{E_a}{h\nu_{\text{laser}}q_{\text{laser}}} = 8.14E_a \quad (12)$$

In Dunbar's model (eq 12),  $\nu_{\text{laser}}$  is the laser frequency (943  $\text{cm}^{-1}$  for a  $\text{CO}_2$  laser), and  $q_{\text{laser}}$  is the laser-frequency single harmonic oscillator partition function, which has values from 1.01 to 1.10 over the range of temperatures of a typical laser dissociation experiment. An average value of 1.05 for  $q_{\text{laser}}$  was used for the working version of Dunbar's model for  $\text{CO}_2$  laser dissociation (eq 12, right-hand side). The activation energy,  $E_a$ , has units of electronvolts (eV) on the right-hand sides of eqs 11 and 12. Our new model predicts that application of the Dunbar model to peptide and protein laser dissociation will result in an underestimation of the activation energy by about 40%.

**Errors.** The laser dissociation model proposed here still has a number of approximations that can lead to errors. Because the right-hand side of eq 7 contains the spontaneous emission term at the laser frequency, the intensity of the laser-frequency transition has an effect on the laser power–temperature relationship. Therefore, an error in the laser-frequency transition dipole moment does not completely drop out of the calculation. However, because the laser-frequency transition dipole moment is often very small for peptides (a value of 0.017 D/mol from the AM1-generated value for LE was used for the above calculations), the spontaneous emission at the laser frequency has a negligible effect on the solution of eq 9. To verify this assumption, the spontaneous emission at the laser frequency was eliminated in a separate calculation. The calculated value of  $s$  changed by less than 1%.

Another potential source of error in our approximation is that the laser-heated ions do not reach a true Boltzmann internal energy distribution. At room temperature, the ion population has a Boltzmann distribution of internal energy. With low-intensity laser heating of the ion population, the internal energy distribution becomes narrower than a Boltzmann distribution.<sup>23</sup> However, a comparison of the internal energy distributions at

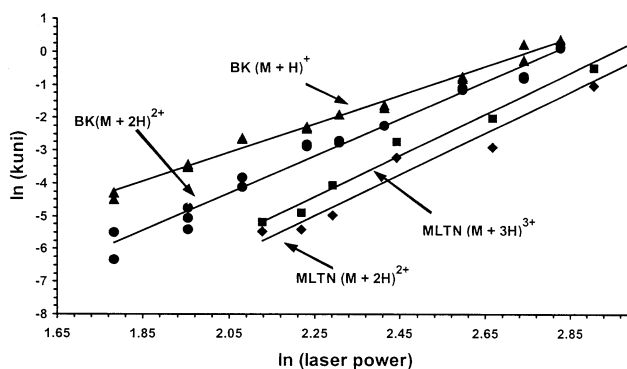


**Figure 4.**  $\text{CO}_2$  laser dissociation data for singly and doubly protonated bradykinin (BK, triangles and circles, respectively) and for doubly and triply protonated melittin (MLTN, diamonds and squares, respectively).

several laser powers shows that the internal energy distribution becomes narrower only very slightly with increasing laser power, and therefore, the primary effect of a narrower distribution should be an underestimation of the laser power necessary to reach an internal energy distribution whose dissociation rate is equal to the dissociation rate of the an ion population with a true Boltzmann internal energy distribution of temperature  $T$ . This increasing underestimation of the laser power necessary to bring molecules to an “effective” temperature  $T$  will result in an underestimation of the activation energy (eq 9). Assessing the magnitude of this error is difficult because the error depends on the threshold dissociation energy and the molecule's rate of radiative energy exchange with the radiation field.

Another assumption of the new laser dissociation model is that the net absorption of the steady-state dissociating ion population is zero. This assumption is valid in the rapid energy exchange limit. Under conditions of fast dissociation, this assumption clearly breaks down. Although we have not estimated the magnitude of the error introduced by neglecting the net absorption of the ion population, it clearly leads to an underestimation of the activation energy.

**Experimental Results and Discussion.** The laser dissociation kinetics of singly and doubly protonated bradykinin and doubly and triply protonated melittin were measured as a function of laser power. The data fit first-order kinetics after a brief induction period during which the ions were brought to a steady-state internal energy distribution.<sup>23</sup> A linear relationship exists between the logarithm of the dissociation rate constant and the logarithm of the laser power for singly and doubly protonated bradykinin and melittin (Figure 4). From the slope of the  $\ln k_{\text{uni}}$  vs  $\ln \rho_{\text{laser}}$  plot, the activation energy can be obtained via eq 11.

The results of the present laser dissociation studies, our previous laser dissociation study of leucine enkephalin,<sup>23</sup> and Freitas et al.'s  $\text{CO}_2$  laser dissociation of bradykinin and bovine ubiquitin<sup>21,22</sup> are shown in Table 2. These results are compared to activation energies measured previously via BIRD.

For leucine enkephalin ( $\text{M} + \text{H}$ )<sup>+</sup>, the smallest ion tested, application of eq 8 to our previous experimental data<sup>23</sup> yields an activation energy of 1.09 eV. This value is nearly identical to the value of 1.1 eV obtained with BIRD.<sup>10</sup> Similarly, the value obtained from our model is very close to that measured by BIRD for doubly protonated bradykinin (0.9 and 0.8 eV, respectively). For bradykinin ( $\text{M} + \text{H}$ )<sup>+</sup>,  $\text{CO}_2$  laser dissociation data measured in our laboratory yield an activation energy via eq 11 that is about 12% lower than the activation energy measured with BIRD (1.16 and 1.3 eV, respectively).<sup>8,9</sup> Freitas et al.<sup>21,22</sup> reported an activation energy of 1.17 eV for singly

**TABLE 2: Comparison of Activation Energies by CO<sub>2</sub> Laser Dissociation with BIRD Derived Activation Energies**

compound	charge state	mass (Da)	$E_a$ (BIRD)	modeled $E_a$ (eV)		
				Dunbar eq 12	this work eq 11	error (% <sup>a</sup> )
leucine enkephalin	1+	555	1.1 <sup>b</sup>	0.66	1.09 <sup>c</sup>	-1
bradykinin	1+	1061	1.3 <sup>d</sup>	0.63	1.16 <sup>e</sup>	-12
bradykinin	1+	1061	1.3 <sup>d</sup>	1.17	1.94 <sup>e</sup>	+49
bradykinin	2+	1061	0.8 <sup>d</sup>	0.50	0.90 <sup>e</sup>	+12
melittin	2+	2845	—	0.77	1.3 <sup>f</sup>	—
melittin	3+	2845	1.76 <sup>g</sup>	0.77	1.3 <sup>f</sup>	—
ubiquitin	5+	8565	1.6 <sup>h</sup>	0.9	1.5 <sup>e</sup>	-7
ubiquitin	11+	8565	1.2 <sup>h</sup>	0.7	1.2 <sup>e</sup>	-3

<sup>a</sup> This work vs BIRD. <sup>b</sup> Schnier et al.<sup>10</sup> <sup>c</sup> See Jockusch et al.<sup>23</sup> <sup>d</sup> Schnier et al.<sup>8</sup> <sup>e</sup> Freitas et al.<sup>22</sup> <sup>f</sup> This study. <sup>g</sup> Busman et al.<sup>25</sup> The dissociation of melittin by Busman et al. was measured by heated metal capillary dissociation. <sup>h</sup> Jockusch et al.<sup>24</sup>

protonated bradykinin using the original Dunbar model (eq 12). This value agrees well with the BIRD measurement of 1.3 eV.<sup>8</sup> However, application of the current model (eq 11) to the laser dissociation data for bradykinin (M + H)<sup>+</sup> measured by Freitas et al. yields an activation energy of 1.94 eV. This value that is significantly larger than that reported here using photodissociation and that obtained previously by BIRD.<sup>8</sup> The reason for this discrepancy in the experimental laser photodissociation data measured by Freitas et al.<sup>21,22</sup> and by us is unknown. Interestingly, Freitas et al. also measured the dissociation of ubiquitin 5+ and 11+ and reported activation energies obtained from the Dunbar model that were much lower than the values from BIRD.<sup>22</sup> However, application of the model presented here to these same data provides activation energy values that are in excellent agreement with BIRD measurements (with errors of less than 10%).

Busman et al. reported a dissociation activation energy of 1.7 eV for triply protonated melittin via heated capillary dissociation.<sup>25</sup> This value is significantly larger than our measurement of 1.3 eV via laser dissociation (Figure 4, Table 2). Similarly high values for the activation energies of protonated leucine enkephalin and leucine enkephalin dimer were reported by Moet-Ner et al.<sup>26</sup> using heated metal capillary dissociation. A possible reason for the high value obtained with this method is interference from ion desolvation.<sup>27</sup> Both the BIRD method and the laser photodissociation method have the advantage that ions are isolated prior to dissociation so that interfering processes, such as ion desolvation, are eliminated.

Overall, the average deviation between activation energies obtained using the current model and BIRD appears to be about 10%. Of course, additional data need to be obtained and analyzed to better estimate the accuracy of this model.

## Conclusions

CO<sub>2</sub> laser dissociation has been applied to the structural elucidation of a wide range of molecules. In combination with the model presented here, this method appears to represent a very promising new technique for the extraction of dissociation activation energies of large molecules. CO<sub>2</sub> laser dissociation has two important advantages over BIRD: First, it is much faster because it does not depend on the lengthy temperature equilibration of the instrument vacuum chamber. Second, CO<sub>2</sub> laser dissociation can access much higher internal energies than BIRD because the only limitation is the maximum available laser power. Biomolecules stable at the highest accessible BIRD temperatures, such as melittin, can easily be dissociated using a CO<sub>2</sub> laser.

The model presented here greatly simplifies the quantitative determination of the activation energy for the dissociation of large ions without full master equation analysis. The current modifications to Dunbar's qualitatively accurate laser dissociation model yield a quantitatively accurate model for peptide and protein laser dissociation. Currently, this laser dissociation model has been applied only to the analysis of peptide and protein dissociation. However, the same model should be equally applicable to all classes of large molecules with very similar absorption spectra (for instance, synthetic polymers or oligonucleotides). For linear polymers, it appears that a simple Arrhenius-like equation relates the experimental laser power-dissociation rate constant relationship to the activation energy for unimolecular dissociation. Therefore, determining the activation energy of large linear polymers should be straightforward from dissociation rate measurements at various laser powers once the appropriate proportionality constant is known. This proportionality constant can readily be calculated, or it can be empirically determined by comparison to BIRD data.

**Acknowledgment.** The authors acknowledge generous financial support from the National Science Foundation (Grant CHE-0098109). The authors also thank Jack Beauchamp for his significant and pioneering contributions in the areas of infrared photodissociation and ion chemistry.

## References and Notes

- Tholmann, D.; Tonner, D. S.; McMahon, T. B. *J. Phys. Chem.* **1994**, *98*, 2002–2004.
- Dunbar, R. C. *J. Phys. Chem.* **1994**, *98*, 8705–8712.
- Dunbar, R. C.; McMahon, T. B.; Tholmann, D.; Tonner, D. S.; Slahub, D. R.; Wei, D. *J. Am. Chem. Soc.* **1995**, *117*, 12819–12825.
- Dunbar, R. C.; McMahon, T. B. *Science* **1998**, *279*, 194–197.
- Price, W. D.; Williams, E. R. *J. Phys. Chem. A* **1997**, *101*, 8844–8852.
- Price, W. D.; Schnier, P. D.; Jockusch, R. A.; Strittmatter, E. F.; Williams, E. R. *J. Am. Chem. Soc.* **1996**, *118*, 10640–10644.
- Price, W. D.; Schnier, P. D.; Williams, E. R. *J. Phys. Chem. B* **1997**, *101*, 664–673.
- Schnier, P. D.; Price, W. D.; Jockusch, R. A.; Williams, E. R. *J. Am. Chem. Soc.* **1996**, *118*, 7178–7189.
- Price, W. D.; Schnier, P. D.; Williams, E. R. *Anal. Chem.* **1996**, *68*, 859–866.
- Schnier, P. D.; Price, W. D.; Strittmatter, E. F.; Williams, E. R. *J. Am. Soc. Mass Spectrom.* **1997**, *8*, 771–780.
- Price, W. D.; Jockusch, R. A.; Williams, E. R. *J. Am. Chem. Soc.* **1997**, *119*, 11988–11989.
- Rodriguez-Cruz, S. E.; Jockusch, R. A.; Williams, E. R. *J. Am. Chem. Soc.* **1998**, *120*, 5842–5843.
- Jockusch, R. A.; Williams, E. R. *J. Phys. Chem. A* **1998**, *102*, 4543–4550.
- Price, W. D.; Jockusch, R. A.; Williams, E. R. *J. Am. Chem. Soc.* **1998**, *120*, 3474–3484.
- Jockusch, R. A.; Price, W. D.; Williams, E. R. *J. Phys. Chem. A* **1999**, *103*, 9266–9274.
- Bomse, D. S.; Woodin, R. L.; Beauchamp, J. L. *J. Am. Chem. Soc.* **1979**, *101*, 5503–5512.
- Thorne, L. R.; Beauchamp, J. L. *J. Chem. Phys.* **1981**, *74*, 5100–5105.
- Dunbar, R. C. *J. Chem. Phys.* **1991**, *95*, 2537–2548.
- Uechi, G. T.; Dunbar, R. C. *J. Chem. Phys.* **1992**, *96*, 8897–8905.
- Dunbar, R. C.; Zaniwski, R. C. *J. Chem. Phys.* **1992**, *96*, 5069–5075.
- Freitas, M. A.; Hendrickson, C. L.; Marshall, A. G. *Rapid Commun. Mass Spectrom.* **1999**, *13*, 1639–1642.
- Freitas, M. A.; Hendrickson, C. L.; Marshall, A. G. *J. Am. Chem. Soc.* **2000**, *122*, 7768–7775.
- Jockusch, R. A.; Paech, K.; Williams, E. R. *J. Phys. Chem. A* **2000**, *104*, 3188–3196.
- Jockusch, R. A.; Schnier, P. D.; Price, W. D.; Strittmatter, E. F.; Demirev, P. A.; Williams, E. R. *Anal. Chem.* **1997**, *69*, 1119–1126.
- Busman, M.; Rockwood, A. L.; Smith, R. D. *J. Phys. Chem.* **1992**, *96*, 2397–2400.
- Moet-Ner, M.; Dongre, A. R.; Somogyi, A.; Wysocki, V. H. *Rapid Commun. Mass Spectrom.* **1995**, *9*, 829–836.
- Schnier, P. D.; Price, W. D.; Strittmatter, E. F.; Williams, E. R. *J. Am. Soc. Mass Spectrom.* **1997**, *8*, 771–780.